Biointerface Research in Applied Chemistry
Open-Access Journal (ISSN: 2069-5837)

Article
Volume 13, Issue 2, 2023, 151
https://doi.org/10.33263/BRIAC132.151

Assessment of Oxidative Stress Effects in Serum Determined by FT-IR Spectroscopy in Cholangiocarcinoma Patients

Huri Bulut [1], Nevzat Tarhan [2], Melek Büyük [3], Kürşat Rahmi Serin [4], Engin Ulukaya [5], Joanna Depciuch [6,*], Magdalena Parlinska-Wojtan [6], Zozan Guleken [7,*]

1 Department of Medical Biochemistry, Faculty of Medicine, Istinye University, 34010, Istanbul, Turkey
2 Uskudar University NP Hospital, Istanbul, Turkey
3 Pathology Department, Faculty of Medicine, Istanbul University, 34390, Istanbul, Turkey
4 Department of General Surgery (Hepatopancreatobiliary Surgery Unit), Faculty of Medicine, Istanbul University, 34390, İstanbul, Turkey
5 Molecular Cancer Research Center (ISUMKAM), Istinye University, Istanbul, Turkey
6 Institute of Nuclear Physics Polish Academy of Science, 31-342 Krakow, Poland; joanna.depciuch@ifj.edu.pl (J.D.);
7 Department of Physiology, Uskudar University Faculty of Medicine, Istanbul, Turkey; zozan.guleken@uskudar.edu (Z.G.);
* Correspondence: zozanguleken@gmail.mail.com (Z.G.); joanna.depciuch@ifj.edu.pl (J.D.);

Scopus Author ID 57118324800
Received: 9.01.2022; Accepted: 5.02.2022; Published: 28.03.2022

Abstract: Cholangiocarcinoma (CCA) is a heterogeneous malignant tumor containing intrahepatic and extrahepatic bile ducts and gallbladder carcinoma. Mostly diagnosed at an advanced stage with a <5% cure chance. Early-stage diagnosis may increase the number of patients who reach curative treatment. Fourier Transform InfraRed (FT-IR) spectroscopy was used to detect chemical changes in serum collected from CCA patients vs. healthy individuals. The study aims to correlate the FTIR spectra with biochemical indices such as TAS, TOS, OSI, and total protein levels. Decreased TAS and increased TOS, OSI, and total protein levels in CCA patients vs. healthy individuals were found. FTIR spectra showed higher absorbance of the peaks corresponding to C–O and bending vibration of C–O–H groups in CCA patients, while more CH_2 functional groups than lipids could be seen in the FTIR spectra of controls serum. PLS analysis showed IR ranges of 1500 cm^{-1} to 1700 cm^{-1}, and 2700 cm^{-1} to 3000 cm^{-1} were able to distinguish between CCA from controls, respectively. PCA confirmed this, while HCA did not differentiate between CCA and those without the disease. Lipids and some functional groups changes caused by oxidative stress can be applied to predict CCA by using FTIR spectroscopy.

Keywords: Cholangiocarcinoma; Fourier Transform InfraRed; oxidative load; total protein.

1. Introduction

Cholangiocarcinoma (CCA) is a highly heterogeneous malignant tumor that can arise at any point in the biliary tract and is asymptomatic at early stages. Recent data reports it accounts for ~15% of all primary liver cancers and ~3% of gastrointestinal malignancies [1,2], and its incidence is increasing globally. The three subtypes of CCA are classified by anatomical origin: intrahepatic (iCCA), extrahepatic (perihilar (pCCA), distal (dCCA)), and gallbladder CA [3,4]. Since they are resistant to chemotherapy and radiotherapy, the only curative treatment is surgery for these malignancies, which have a poor prognosis. This approach is only possible for localized, early-stage diseases. Early diagnosis is difficult due to the

asymptomatic course at early stages, the onset of symptoms at an advanced stage, lack of accurate diagnostic tests, and low specificity and sensitivity of imaging modalities. Definitive diagnosis is usually made with high suspicion of clinical, laboratory, endoscopic and radiological findings, even in most advanced tumors [5].

Proteins, carbohydrates, lipids, and nucleic acids circulating from cells are promising diagnostic and prognostic tools for human diseases [6,7]; Its basis is to use the differentiation of biomacromolecules to diagnose different types of cancer. Proteins that are dysregulated in cancer cells are involved in processes such as DNA repair, cell proliferation differentiation, cell cycle regulation, cell death, organ development, and stress response [8]. One of the key features of cancer cells is altered lipid metabolism. Modulating certain enzymes results in the accumulation of material that promotes and accelerates growth [9]; These marked changes in growth suggest that some lipids may be used as cancer biomarkers [10]. Metabolic reactions are also very important in cancer cells. Metabolic reactions that can be classified as anabolic or catabolic include synthesis and degradation reactions of compounds such as proteins, carbohydrates, lipids, and nucleic acids. These metabolic reactions can generate free radicals/reactive oxygen species (ROS) via oxidative phosphorylation [11]. ROS production is associated with activating certain signaling pathways that trigger cancer initiation, apoptosis, and cancer progression and affect cell survival [12]. Depending on its concentration, ROS can influence cancer progression by initiating/stimulating oncogenesis, promoting the transformation/proliferation of cancer cells, or causing cell death [13]. Excessive production of ROS in cells also damages cell components such as lipids, proteins, DNA, carbohydrates, and enzymes, causing cancer, heart diseases, intestinal diseases, depression, vascular disorders, and premature aging [14].

Given that the metabolism of cancer cells differs from that of normal cells and describes the metabolic process of CCA, the study compared serum assays of CCA patients with those of healthy individuals; For this, total antioxidant status (TAS) and total oxidant status (TOS) levels and calculated oxidative stress indices (OSI) were used. The study also measured and compared the total protein concentrations of CCA patients and healthy controls and measured CA19-9 [15]. Finally, the study used Fourier transform infrared (FT-IR) spectroscopy, a powerful technique for detecting the absorption of molecular vibrations [16-18], to identify chemical changes in serum caused by CCA, and explored FTIR spectra together with multivariate analyzes such as PLS, PCA. HCA as a diagnostic tool of CCA.

2. Materials and Methods

2.1. Serum samples.

Istinye University, Medical Faculty Clinical Research Ethics Committee approval was obtained (date: 15.09.2021, number: 2017-KAEK-120)/2/2021.G-138). CCA patients (n:29) and healthy individuals (n:26) were included in the study who applied to the General Surgery Department of Istanbul University Faculty of Medicine. The inclusion criteria for the study were patients older than 18 years of age, histopathological confirmation of the diagnosis CCA, level of CA 19-9 $\geq$ 100 or FISH polysomy positivity, and detected mass lesion by imaging methods [19]. The control group included healthy individuals between 18-65 years old without a cancer diagnosis and hormonal, chronic, and connective tissue diseases.

2.2. Total Protein, TAS, and TOS measurements in serum samples.

Total protein in serum samples was measured based on the Bradford method [20,21], and serial dilutions of bovine serum albumin (BSA) were prepared as standard as 1 mg/ml solutions. Results were obtained at 595 nm on a microplate reader (Thermo Scientific Multiskan FC, 2011-06, USA).

Total Antioxidant Status (TAS) and Total Oxidant Status (TOS) levels were measured by spectrophotometry using a commercial kit (Rel Assay, Turkey). Results were expressed in μm H_2O_2 Equiv/L and Trolox.equiv/L for TOS and TAS, respectively. TAS levels were calculated according to the formula: (ΔAbs Std1)- (ΔAbs example)/ (ΔAbs Std1) -(ΔAbs Std2), while the TOS levels were calculated by using (ΔAbs Sample/ ΔAbs standard2) x 20 (standard 2) formula. Oxidative stress index (OSI) values were obtained by TOS/ TAS ratio.

2.3. FTIR measurements.

The study used Bruker's Vertex 70v spectrometer with attenuated total reflection (ATR) diamond crystal plate to measure the absorbance spectra of serum samples, using an IR range between 400 cm^{-1} and 4000 cm^{-1} and 32 scans with spectral resolution 4 cm^{-1}. Collected blood samples were centrifuged (15 min., 3000 rpm), and the serum was separated and stored (-80°C). Before FTIR measurement, samples were defrosted, spotted on a CaF_2 slide, and dried. The device's ATR crystal was washed between measurements of each sample [22]. After measurement, all spectra were analyzed using OPUS 7.0 software. Baseline correction, vector normalization, and 9 smoothed with Savitzky–Golay was performed [23,24].

2.4. Multivariate analysis of FTIR spectra.

To ascertain the similarity of CCA serum to CCA-free serum and the possibility of distinguishing CCA using FTIR spectroscopy, Principal Component Analysis (PCA) and Hierarchical Component Analysis (HCA) were performed. To determine wave numbers that could differentiate CCA serum from CCA-free serum, PCA and HCA analyses were performed using Past 3.0. software and PLS using Origin 2019 software; PCA and HCA addressed the 800 cm^{-1} to 1800 cm^{-1} range and PLS analysis 600 cm^{-1} to 3500 cm^{-1} range. PLS analysis addressed intermediary ranges [25,26].

2.5. Statistical analysis.

The study used the Statistical Package for Social Sciences (SPSS), version 20.0, for analysis; $P<0.05$ was significant. The unpaired Student t-test was used to compare the two groups. Using results showing mean ± SD, a one-way analysis of variance (ANOVA) followed by multiple comparisons with Tukey's post hoc test was performed.

3. Results and Discussion

Biochemical parameters differ significantly between CCA patients and healthy individuals. The differences are summarized in figures 1 and 2.

To evaluate the metabolic process in serum samples collected from CCA and healthy individuals, total protein, TAS, TOS values were measured, and OSI values were calculated. As shown in Figure 1, TAS value (0.777±0.0457) was significantly lower ($p < 0.001$) in CCA patients compared to controls (1.58±0.237), while TOS levels (9.73±1.46) were significantly

higher than controls (4.06±0.325), as an expected finding ($p < 0.001$). We calculated the OSI values indicating the corresponding antioxidant level per unit oxidant molecule and found them significantly higher in the CCA group (12.6±2.39) than controls (2.63±0.396).

Total protein levels were significantly increased in the CCA group (5.51±0.676) compared to controls (1.79±0.403) ($p<0.001$) shown in Figure 2.

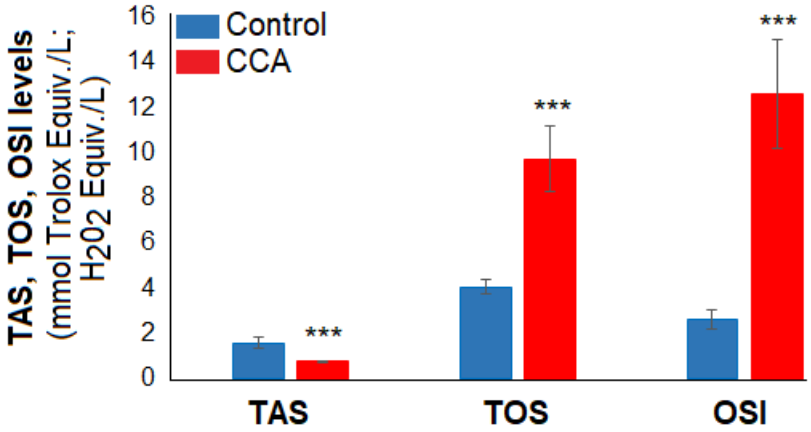

Figure 1. Comparison of TOS, OSI, TAS levels in cholangiocarcinoma patients (CCA) and controls (*** is noted as $p<0.001$).

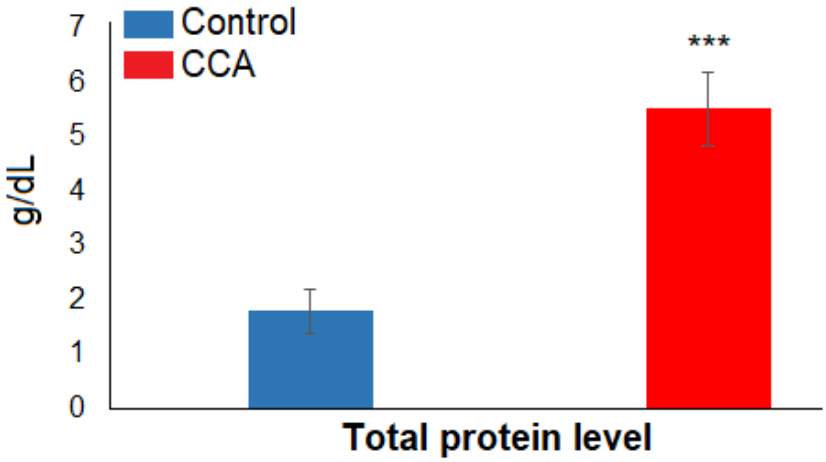

Figure 2. Comparison of total protein value in cholangiocarcinoma patients (CCA) and controls (*** is noted as $p<0.001$).

Figure 3 shows FTIR spectra representing differences in the chemical compositions of the serum collected from the two analyzed groups. Peaks at 1082 cm^{-1} and 1165 cm^{-1} corresponded to C–O vibration and C–O–H group bending vibration [27,28]. Amide vibrations (amide III, amide II, and amide I) appeared at wavenumbers 1238 cm^{-1} and 1304 cm^{-1}, 1531 $cm^{-1,}$ and 1635 cm^{-1} [29]. C=O vibration at wavenumber 1392 cm^{-1} was marked by a peak at 1454 cm^{-1} from C–H stretching vibrations [30]. Peaks around 3278 cm^{-1} originated from O–H stretching vibrations. Peaks at wavenumbers 2958 cm^{-1}, 2931 $cm^{-1,}$ and 2872 cm^{-1} originated from asymmetric vibration of C–H in CH_3, asymmetric vibration of C–H in CH_2, and symmetric vibration of C–H in CH_3 [31].

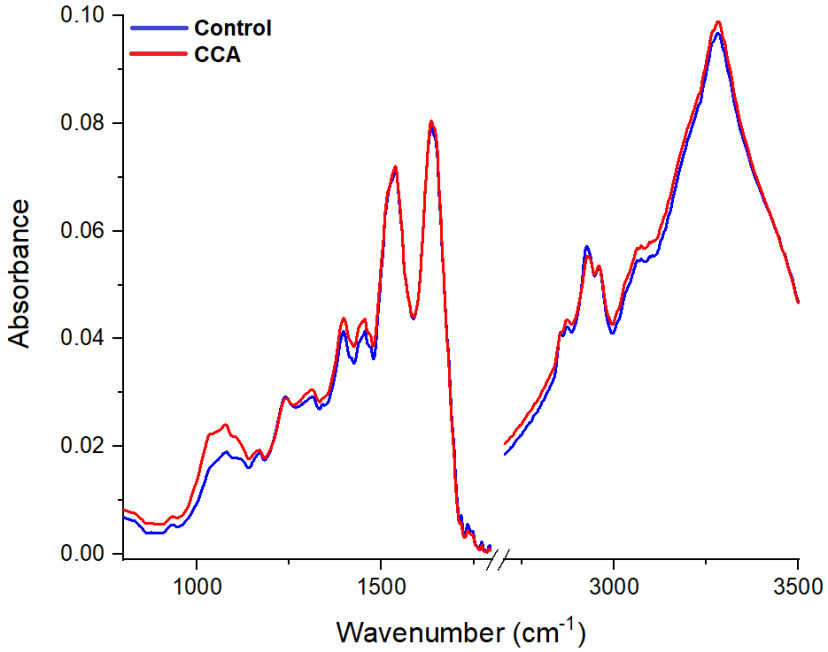

Figure 3. FTIR spectra of serum collected from CCA (red spectrum) patients and controls (blue spectrum).

The obtained spectra showed differences in the absorbance values of the two analyzed groups. Comparing the CCA spectrum to the control spectrum, higher peak absorbance corresponding to C–O and bending vibration of C–O–H groups was observed. Furthermore, little increase in absorbance was seen in the CCA spectrum at wavenumbers 1392 cm^{-1} and 1454 cm^{-1}, while the control spectra showed higher amounts of CH_2 functional groups from lipids.

To investigate FTIR spectroscopy as a diagnostic tool in cancer, disorders and other diseases, the study explored FTIR spectroscopy as a method for CCA diagnosis. For this, multivariate analyses were performed.

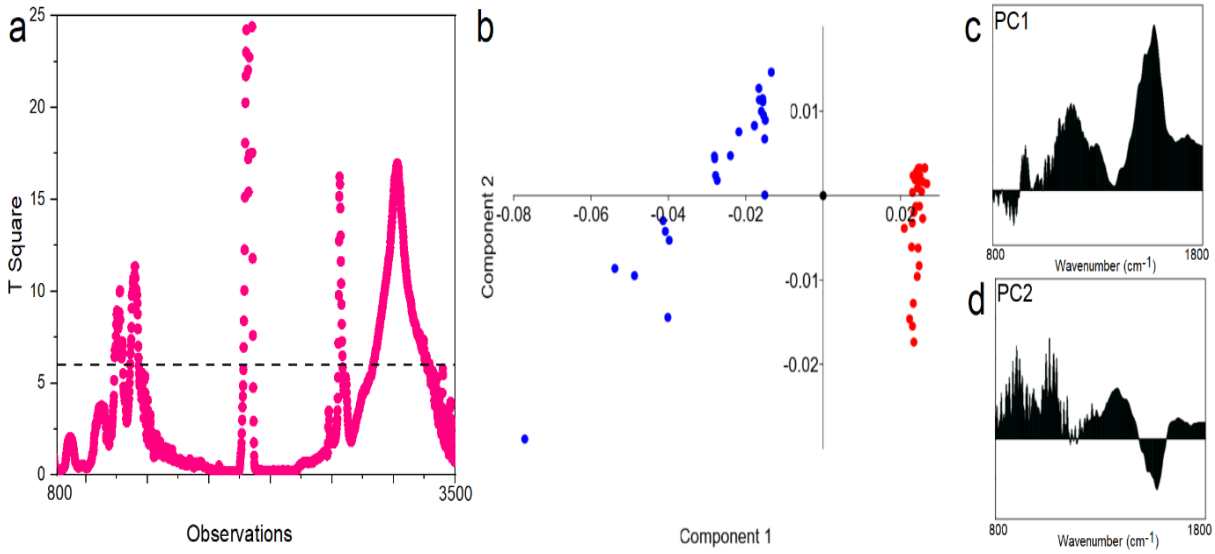

Figure 4. PLS analysis of IR range 600 - 3500 cm^{-1} (a); PCA analysis of IR range 800 - 1800 cm^{-1} (b) of serum collected from control (blue dot) and CCA (red dot) patients with PC1 (c) and PC2 (d) loading.

The PLS analysis presented in Figure 4a shows an IR range of 1500 - 1700 cm^{-1}, corresponding to amide II and amide I vibrations. Wavenumbers around 2900 cm^{-1} were placed under the line of significance. These wavenumber values distinguish CCA serum samples from

CCA-free serum samples. In addition, PCA analysis in Figure 4b shows FTIR spectroscopy to distinguish CCA serum samples from CCA-free serum samples; here, the PC1 component is most important in showing negative values for controls and positive values for CCA patients. Loading plots presented in Figures 4c and 4d show positive PC1 values in wavenumbers of 1000-1600 cm^{-1} and negative PC2 values in wavenumbers of 1400-1500 cm^{-1}.

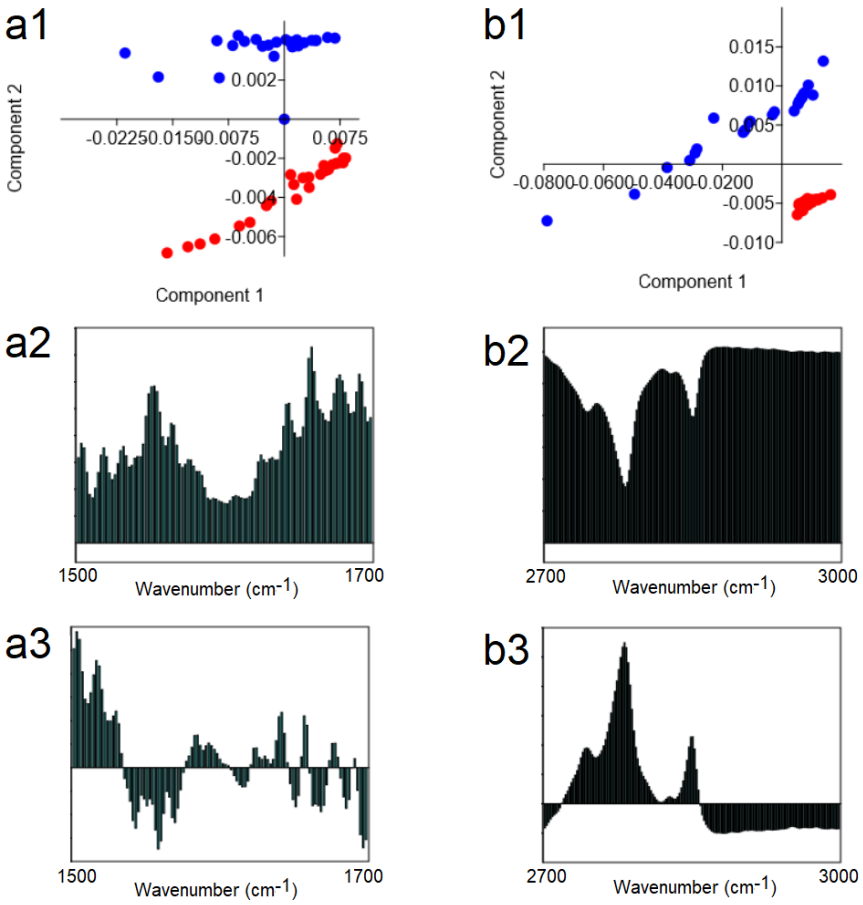

Figure 5. PCA analysis of IR from serum collected from CCA (red dot) patients and controls (blue dot), with PC1 (a2, b2) and PC2 (a3, b3) loading.

Figure 5a1 presents PCA analysis of IR range 1500 - 17000 cm^{-1}. The IR of amide II and amide I vibrations can be seen to distinguish CCA serum from control serum. In this range, CCA samples were placed in negative values, and control samples were placed in positive values of PC1 component. Figure 5a2 presents the loading plot of the PC1 component of amide vibrations, showing positive values in all ranges. Figure 5a3 shows the PC2 component had negative values at wavenumbers between 1550 cm^{-1} and 1575 cm^{-1} and between 1640 cm^{-1} and 1700 cm^{-1}. In addition, Figure 5b1 presents the IR range corresponding to CH vibrations from lipids, which can be seen to differentiate CCA serum collected from the control serum. All CCA samples were placed in the same quadrants of the coordinate system, assuming positive values for the PC1 component and negative values for the PC2 component. Figure 5b2 shows the loading plot values of the PC1 component to be positive in all analyzed lipid FTIR ranges and the loading plot values of the PC2 component to be negative from wavenumber 2850 cm^{-1}.

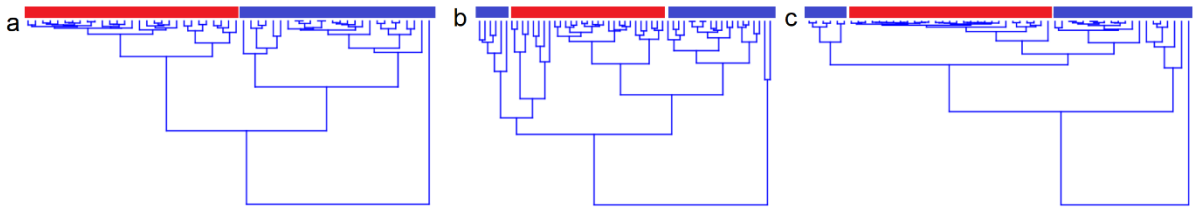

Figure 6. HCA analysis of IR range 800 - 1800 cm^{-1} (a); 1500 - 17000 cm^{-1} (b); and 2700 - 3000 cm^{-1} (c) of serum collected from control (blue) and CCA (red) patients.

HCA analysis of IR range 800 - 1800 cm^{-1} distinguished two separate yet similar groups, one created from CCA serum samples and the other from controls. These are presented in Figure 6a. In the case of selective IR range (1500 cm^{-1} and 17000 cm^{-1} and between 2700 cm^{-1} and 3000 cm^{-1}, Figures 6b and 6c, respectively), the similarity group created from healthy individuals collected from healthy individuals was divided into two parts. All CCA samples obtained from CCA patients still created one group of similarities.

Cholangiocarcinoma is cancer diagnosed in advanced stages with poor prognoses and a <5% cure rate. In the early stage, CCA is usually asymptomatic [3,32,33]. Therefore, an effective, feasible, simple diagnostic test is necessary for the early diagnosis of CCA. FTIR is a spectroscopy method that provides information about the chemical composition of serum samples [34,35]. Via FTIR, it visualizes possible changes caused by changes in serum samples, e.g., drugs and diseases [36]. This study performed a multivariate analysis of data from FTIR spectroscopy to identify CCA-induced chemical changes and investigate FTIR spectroscopy as a diagnostic tool in CCA. The FTIR spectra in Figure 3 show more functional groups with glucose vibrations in CCA serum than in control serum. During cancer progression, changes in metabolism may include sugar backbone alterations [37], glycogen degradation, or changes in the by-products of glucose consumption [38]. FTIR spectra changes reflect these processes. The analyzed FTIR range of 1000 - 1150 cm^{-1} differed between the CCA and control groups and made visible vibrations of functional group formation of collagen; This is important because changes in collagen, particularly collagen release from the tumor microenvironment, may signal cancer progression and make collagen a prognostic indicator for cancer [39]. Prakobwong et al. showed a significant increase in type I collagen in CCA plasma compared to healthy patients [40]; this phenomenon can be seen in Figure 3. The results of the PLS and PCA analyses in Figures 4 and 5a1 showed that the amide I and II regions differentiated CCA serum from control serum. Indeed, molecular results showed that specific proteins presented spectral signatures in CCA serum [40]. The multivariate analysis presented in Figures 5b1 and 6c shows that lipid IR regions differentiate CCA serum from controls. Lipids are building blocks for cell membranes and facilitate signaling between cells. Cancer and other cells in the tumor microenvironment appropriate lipids, changing their metabolism to achieve a plastic and context-dependent metabolic reprogramming driven by oncogenic and environmental cues. These and other changes in lipid composition and structure permit cancer cells to thrive in a changing microenvironment, supporting the development of cancer and oncogenic functions of cancer cells [41].

However, in some studies on other types of cancer, very similar results were obtained using FTIR spectroscopy, as in the case of CCA. In brain cancer, the changes in the amide's region, which can be used to distinguish cancer and noncancer tissues, were visible [42]. In some types of gastric cancer, changes in the same region as observed in this study were found [8]. Therefore, in addition to the use of standard medical diagnostic tools, the use of FTIR can

help diagnose CCA. We showed the increased levels of TOS, OSI, and total protein in serum from the CCA patients in our study. Such increases suggest the presence of inflammation, possibly from cancer [28].

4. Conclusions

This study shows that FTIR spectroscopy, combined with multivariate analysis, distinguishes the serum samples of people with CCA from healthy individuals. FTIR spectra of serum collected from CCA patients showed higher absorbance of peaks at wavelengths 1082 cm-1, 1165 cm^{-1}, 1392 cm^{-1}, and 1454 cm^{-1} corresponding to C–O, bending vibration of C–O–H groups and C=O groups. In addition, serum collected from CCA patients showed decreased absorbance of CH2 functional groups from lipids. PLS analysis revealed differences in sera collected from CCA patients and healthy individuals in IR ranges 1500-1700 cm^{-1} and 2700-3000 cm^{-1}. Performed PCA analysis confirmed this result. HCA analysis of samples collected from CCA patients and healthy individuals identified characteristics specific to each group. Furthermore, biochemical results showed higher TOS, OSI, and total protein levels in CCA patients and lower levels of TAS in healthy individuals. This study shows that FTIR spectroscopy, combined with PLS, PCA, HCA analysis, and biochemical assays, can differentiate the serum of CCA patients from that of healthy individuals.

Funding

This research received no external funding.

Acknowledgments

This research has no acknowledgment.

Conflicts of Interest

The authors declare no conflict of interest.

References

1. DeOliveira, M.L.; Cunningham, S.C.; Cameron, J.L.; Kamangar, F.; Winter, J.M.; Lillemoe, K.D.; Choti, M.A.; Yeo, C.J.; Schulick, R.D. Cholangiocarcinoma: Thirty-One-Year Experience with 564 Patients at a Single Institution. *Ann Surg* **2007**, *245*, 755–762, https://doi.org/10.1097/01.sla.0000251366.62632.d3.
2. Banales, J.M.; Cardinale, V.; Carpino, G.; Marzioni, M.; Andersen, J.B.; Invernizzi, P.; Lind, G.E.; Folseraas, T.; Forbes, S.J.; Fouassier, L.; Geier, A.; Calvisi, D.F.; Mertens, J.C.; Trauner, M.; Benedetti, A.; Maroni, L.; Vaquero, J.; Macias, R.I.; Raggi, C.; Perugorria, M.J.; Gaudio, E.; Boberg, K.M.; Marin, J.J.; Alvaro, D. Expert consensus document: Cholangiocarcinoma: current knowledge and future perspectives consensus statement from the European Network for the Study of Cholangiocarcinoma (ENS-CCA). *Nature reviews. Gastroenterology & hepatology* **2016**, *13*, 261-280, https://doi.org/10.1038/nrgastro.2016.51.
3. Banales, J.M.; Marin, J.J.G.; Lamarca, A.; Rodrigues, P.M.; Khan, S.A.; Roberts, L.R.; Cardinale, V.; Carpino, G.; Andersen, J.B.; Braconi, C.; Calvisi, D.F.; Perugorria, M.J.; Fabris, L.; Boulter, L.; Macias, R.I.R.; Gaudio, E.; Alvaro, D.; Gradilone, S.A.; Strazzabosco, M.; Marzioni, M.; Coulouarn, C.; Fouassier, L.; Raggi, C.; Invernizzi, P.; Mertens, J.C.; Moncsek, A.; Rizvi, S.; Heimbach, J.; Koerkamp, B.G.; Bruix, J.; Forner, A.; Bridgewater, J.; Valle, J.W.; Gores, G.J. Cholangiocarcinoma 2020: The next Horizon in Mechanisms and Management. *Nat Rev Gastroenterol Hepatol* **2020**, *17*, 557–588, https://doi.org/10.1038/s41575-020-0310-z.
4. Blechacz, B.; Komuta, M.; Roskams, T.; Gores, G.J. Clinical Diagnosis and Staging of Cholangiocarcinoma. *Nat Rev Gastroenterol Hepatol* **2011**, *8*, 512–522, https://doi.org/10.1038/nrgastro.2011.131.
5. Komuta, M.; Yeh, M.M. A Review on the Update of Combined Hepatocellular Cholangiocarcinoma. *Semin Liver Dis* **2020**, *40*, 124–130, https://doi.org/10.1055/s-0039-3402515.

6. Andersen, R.F.; Jakobsen, A. Screening for Circulating RAS/RAF Mutations by Multiplex Digital PCR. *Clin Chim Acta* **2016**, *458*, 138–143, https://doi.org/10.1016/j.cca.2016.05.007.
7. Macias, R.I.R.; Banales, J.M.; Sangro, B.; Muntané, J.; Avila, M.A.; Lozano, E.; Perugorria, M.J.; Padillo, F.J.; Bujanda, L.; Marin, J.J.G. The Search for Novel Diagnostic and Prognostic Biomarkers in Cholangiocarcinoma. *Biochim Biophys Acta Mol Basis Dis* **2018**, *1864*, 1468–1477, https://doi.org/10.1016/j.bbadis.2017.08.002.
8. Guleken, Z.; Bulut, H.; Gültekin, G.İ.; Arıkan, S.; Yaylım, İ.; Hakan, M.T.; Sönmez, D.; Tarhan, N.; Depciuch, J. Assessment of Structural Protein Expression by FTIR and Biochemical Assays as Biomarkers of Metabolites Response in Gastric and Colon Cancer. *Talanta* **2021**, *231*, https://doi.org/10.1016/j.talanta.2021.122353.
9. Pradas, I.; Huynh, K.; Cabré, R.; Ayala, V.; Meikle, P.J.; Jové, M.; Pamplona, R. Lipidomics Reveals a Tissue-Specific Fingerprint. *Frontiers in Physiology* **2018**, *9*, https://doi.org/10.3389/fphys.2018.01165.
10. Szlasa, W.; Zendran, I.; Zalesińska, A.; Tarek, M.; Kulbacka, J. Lipid Composition of the Cancer Cell Membrane. *J Bioenerg Biomembr* **2020**, *52*, 321–342, https://doi.org/10.1007/s10863-020-09846-4.
11. Liou, G.-Y.; Storz, P. Reactive Oxygen Species in Cancer. *Free Radic Res* **2010**, *44*, 479–496, https://doi.org/10.3109/10715761003667554.
12. Khan, M.A.; Tania, M.; Zhang, D.; Chen, H. Antioxidant Enzymes and Cancer. *Chinese Journal of Cancer Research* **2010**, *22*, 87–92, https://doi.org/10.1007/s11670-010-0087-7.
13. Hayes, J.D.; Dinkova-Kostova, A.T.; Tew, K.D. Oxidative Stress in Cancer. *Cancer Cell* **2020**, *38*, 167–197, https://doi.org/10.1016/j.ccell.2020.06.001.
14. Vander Heiden, M.G.; Cantley, L.C.; Thompson, C.B. Understanding the Warburg Effect: The Metabolic Requirements of Cell Proliferation. *Science* **2009**, *324*, 1029–1033, https://doi.org/10.1126/science.1160809.
15. Rodrigues, P.M.; Olaizola, P.; Paiva, N.A.; Olaizola, I.; Agirre-Lizaso, A.; Landa, A.; Bujanda, L.; Perugorria, M.J.; Banales, J.M. Pathogenesis of Cholangiocarcinoma. *Annu Rev Pathol* **2021**, *16*, 433–463, https://doi.org/10.1146/annurev-pathol-030220-020455.
16. Güleken, Z.; Ünübol, B.; Toraman, S.; Bilici, R.; Gündüz, O.; Kuruca, S.E. Diagnosis of Opioid Use Disorder with High Sensitivity and Specificity by Advanced Computational Analysis of Fourier Transform Infrared Spectroscopy. *Infrared Physics & Technology* **2020**, *105*, https://doi.org/10.1016/j.infrared.2020.103218.
17. Guleken, Z.; Ünübol, B.; Bilici, R.; Sarıbal, D.; Toraman, S.; Gündüz, O.; Erdem Kuruca, S. Investigation of the Discrimination and Characterization of Blood Serum Structure in Patients with Opioid Use Disorder Using IR Spectroscopy and PCA-LDA Analysis. *Journal of Pharmaceutical and Biomedical Analysis* **2020**, *190*, https://doi.org/10.1016/j.jpba.2020.113553.
18. Guleken, Z.; Jakubczyk, P.; Wiesław, P.; Krzysztof, P.; Bulut, H.; Öten, E.; Depciuch, J.; Tarhan, N. Characterization of Covid-19 Infected Pregnant Women Sera Using Laboratory Indexes, Vibrational Spectroscopy, and Machine Learning Classifications. *Talanta* **2022**, *237*, https://doi.org/10.1016/j.talanta.2021.122916.
19. Nault, J.-C.; Villanueva, A. Biomarkers for Hepatobiliary Cancers. *Hepatology* **2021**, *73 Suppl 1*, 115–127, https://doi.org/10.1002/hep.31175.
20. Guleken, Z.; Kuruca, S.E.; Ünübol, B.; Toraman, S.; Bilici, R.; Sarıbal, D.; Gunduz, O.; Depciuch, J. Biochemical Assay and Spectroscopic Analysis of Oxidative/Antioxidative Parameters in the Blood and Serum of Substance Use Disorders Patients. A Methodological Comparison Study. *Spectrochimica Acta Part A: Molecular and Biomolecular Spectroscopy* **2020**, *240*, https://doi.org/10.1016/j.saa.2020.118625.
21. Kruger, N.J. The Bradford Method for Protein Quantitation. *Methods Mol Biol* **1994**, *32*, 9–15, https://doi.org/10.1385/0-89603-268-X:9.
22. Chatchawal, P.; Wongwattanakul, M.; Tippayawat, P.; Kochan, K.; Jearanaikoon, N.; Wood, B.R.; Jearanaikoon, P. Detection of Human Cholangiocarcinoma Markers in Serum Using Infrared Spectroscopy. *Cancers (Basel)* **2021**, *13*, https://doi.org/10.3390/cancers13205109.
23. Guleken, Z.; Depciuch, J.; Ege, H.; İlbay, G.; Kalkandelen, C.; Ozbeyli, D.; Bulut, H.; Sener, G.; Tarhan, N.; Erdem Kuruca, S. Spectrochemical and Biochemical Assay Comparison Study of the Healing Effect of the Aloe Vera and Hypericum Perforatum Loaded Nanofiber Dressings on Diabetic Wound. *Spectrochimica Acta Part A: Molecular and Biomolecular Spectroscopy* **2021**, *254*, https://doi.org/10.1016/j.saa.2021.119639.
24. Guleken, Z.; Bulut, H.; Depciuch, J.; Tarhan, N. Diagnosis of Endometriosis Using Endometrioma Volume and Vibrational Spectroscopy with Multivariate Methods as a Noninvasive Method. *Spectrochimica Acta Part A: Molecular and Biomolecular Spectroscopy* **2022**, *264*, https://doi.org/10.1016/j.saa.2021.120246.
25. Sim, S.F.; Jeffrey Kimura, A.L. Partial Least Squares (PLS) Integrated Fourier Transform Infrared (FTIR) Approach for Prediction of Moisture in Transformer Oil and Lubricating Oil. *Journal of Spectroscopy* **2019**, *2019*, https://doi.org/10.1155/2019/5916506.
26. Yang, C.M.; Shu, J. Cholangiocarcinoma Evaluation via Imaging and Artificial Intelligence. *Oncology* **2021**, *99*, 72–83, https://doi.org/10.1159/000507449.
27. Zou, Y.; Xia, P.; Yang, F.; Cao, F.; Ma, K.; Mi, Z.; Huang, X.; Cai, N.; Jiang, B.; Zhao, X.; Liu, W.; Chen, X. Whole blood and semen identification using mid-infrared and Raman spectrum analysis for forensic applications. *Analytical Methods* **2016**, *8*, 3763-3767, https://doi.org/10.1039/C5AY03337C.

28. Ji, Y.; Yang, X.; Ji, Z.; Zhu, L.; Ma, N.; Chen, D.; Jia, X.; Tang, J.; Cao, Y. DFT-Calculated IR Spectrum Amide I, II, and III Band Contributions of N-Methylacetamide Fine Components. *ACS Omega* **2020**, *5*, 8572–8578, https://doi.org/10.1021/acsomega.9b04421.
29. Shao, D.; Wei, Q. Microwave-Assisted Rapid Preparation of Nano-ZnO/Ag Composite Functionalized Polyester Nonwoven Membrane for Improving Its UV Shielding and Antibacterial Properties. *Materials (Basel)* **2018**, *11*, https://doi.org/10.3390/ma11081412.
30. Derenne, A.; Claessens, T.; Conus, C.; Goormaghtigh, E. Infrared Spectroscopy of Membrane Lipids. In: *Encyclopedia of Biophysics*. Roberts, G.C.K. Ed.; Springer: Berlin, Heidelberg, **2013**; pp. 1074–1081, https://doi.org/10.1007/978-3-642-16712-6_558.
31. Analytical Methods Committee, A.N. Fourier transform infrared spectroscopic analysis of organic archaeological materials: background paper. *Analytical Methods* **2021**, *13*, 2997-3000, https://doi.org/10.1039/D1AY90064A.
32. Su, K.-Y.; Lee, W.-L. Fourier Transform Infrared Spectroscopy as a Cancer Screening and Diagnostic Tool: A Review and Prospects. *Cancers (Basel)* **2020**, *12*, https://doi.org/10.3390/cancers12010115.
33. Boonsri, B.; Choowongkomon, K.; Kuaprasert, B.; Thitiphatphuvanon, T.; Supradit, K.; Sayinta, A.; Duangdara, J.; Rudtanatip, T.; Wongprasert, K. Probing the Anti-Cancer Potency of Sulfated Galactans on Cholangiocarcinoma Cells Using Synchrotron FTIR Microspectroscopy, Molecular Docking, and In Vitro Studies. *Mar Drugs* **2021**, *19*, https://doi.org/10.3390/md19050258.
34. Fabris, L.; Sato, K.; Alpini, G.; Strazzabosco, M. The Tumor Microenvironment in Cholangiocarcinoma Progression. *Hepatology* **2021**, *73 Suppl 1*, 75–85, https://doi.org/10.1002/hep.31410.
35. Bergquist, J.R.; Ivanics, T.; Storlie, C.B.; Groeschl, R.T.; Tee, M.C.; Habermann, E.B.; Smoot, R.L.; Kendrick, M.L.; Farnell, M.B.; Roberts, L.R.; Gores, G.J.; Nagorney, D.M.; Truty, M.J. Implications of CA19-9 elevation for survival, staging, and treatment sequencing in intrahepatic cholangiocarcinoma: A national cohort analysis. *Journal of Surgical Oncology* **2016**, *114*, 475-482, https://doi.org/10.1002/jso.24381.
36. Zois, C.E.; Harris, A.L. Glycogen Metabolism Has a Key Role in the Cancer Microenvironment and Provides New Targets for Cancer Therapy. *J Mol Med (Berl)* **2016**, *94*, 137–154, https://doi.org/10.1007/s00109-015-1377-9.
37. Brassart-Pasco, S.; Brézillon, S.; Brassart, B.; Ramont, L.; Oudart, J.-B.; Monboisse, J.C. Tumor Microenvironment: Extracellular Matrix Alterations Influence Tumor Progression. *Front Oncol* **2020**, *10*, https://doi.org/10.3389/fonc.2020.00397.
38. Chatchawal, P.; Wongwattanakul, M.; Tippayawat, P.; Kochan, K.; Jearanaikoon, N.; Wood, B.R.; Jearanaikoon, P. Detection of Human Cholangiocarcinoma Markers in Serum Using Infrared Spectroscopy. *Cancers (Basel)* **2021**, *13*, https://doi.org/10.3390/cancers13205109.
39. De Bruyne, S.; Speeckaert, M.M.; Delanghe, J.R. Applications of Mid-Infrared Spectroscopy in the Clinical Laboratory Setting. *Crit Rev Clin Lab Sci* **2018**, *55*, 1–20, https://doi.org/10.1080/10408363.2017.1414142.
40. Butler, L.M.; Perone, Y.; Dehairs, J.; Lupien, L.E.; de Laat, V.; Talebi, A.; Loda, M.; Kinlaw, W.B.; Swinnen, J.V. Lipids and Cancer: Emerging Roles in Pathogenesis, Diagnosis and Therapeutic Intervention. *Adv Drug Deliv Rev* **2020**, *159*, 245–293, https://doi.org/10.1016/j.addr.2020.07.013.
41. Depciuch, J.; Tołpa, B.; Witek, P.; Szmuc, K.; Kaznowska, E.; Osuchowski, M.; Król, P.; Cebulski, J. Raman and FTIR Spectroscopy in Determining the Chemical Changes in Healthy Brain Tissues and Glioblastoma Tumor Tissues. *Spectrochim Acta A Mol Biomol Spectrosc* **2020**, *225*, https://doi.org/10.1016/j.saa.2019.117526.
42. Tutuncu, E.O.; Dundar, Z.D.; Kilinc, I.; Tutuncu, A.; Kocak, S.; Girisgin, A.S. Prognostic Value of Immunosuppressive Acidic Protein and Oxidative Stress Status in Critically Ill Patients. *Indian J Crit Care Med* **2021**, *25*, 405–409, https://doi.org/10.5005/jp-journals-10071-23788.